Supporting Information

Graphite-Conjugated Pyrazines as Molecularly Tunable Heterogeneous Electrocatalysts

Tomohiro Fukushima,[§] Walter Drisdel,[†] Junko Yano,[†#] Yogesh Surendranath[§,*]

[§] Department of Chemistry, Massachusetts Institute of Technology,

Cambridge, Massachusetts 02139, United States

[†] Joint Center for Artificial Photosynthesis, Lawrence Berkeley National Laboratory,

Berkeley, California, 94720, United States.

[#]Physical Biosciences Division, Lawrence Berkeley National Laboratory,

Berkeley, California, 94720, United States.

yogi@mit.edu

Table of contents

Experimental Methods

Chemicals and Materials. Potassium hydroxide (99.99%, semiconductor grade), NaOH (99.99%, semiconductor grade), tetrabutylammonium hexafluorophosphate (99%), 4-fluoro-1,2-phenylenediamine (97%), 3,4-diaminotoluene (99%), di-*tert*-butyl dicarbonate (ReagentPlus® 99%), 1-chloro-2,4-dinitrobenzene, (>99%), 4-fluoroaniline (97%), 2,2,2-trifluoroethanol (ReagentPlus®, 99%), 9,10-phenanthrenequinone (95%), phenazine (98%), 3,4-diaminobenzenecarboxylic acid (97%), trifluoroacetic acid (ReagentPlus® 99%), 3,4-diaminopyridine, and Nafion® perfluorinated resin 5wt% solution were obtained from Sigma Aldrich and were used as received. $CdSO_4 \cdot 3H_2O$ (99.996%) was obtained from Alfa Aesar and used as received. All syntheses were performed in solvent of ACS grade. All aqueous electrolyte solutions were prepared with reagent grade water (Millipore, 18.2 MΩ-cm resistivity). Chelex® 100 Resin was obtained from Bio-Rad (Catalog # 210011676). Acetonitrile (ACS grade, Aldrich) was used without further purification for the preparation of all non-aqueous electrolytes. Glassy carbon disk electrodes were obtained from Pine Research Instrumentation, Inc. Hg/HgO and Ag/AgCl reference electrodes were obtained from CHI instruments, Inc. and BASi Inc. respectively. Monarch 1300 was obtained from Cabot. Platinum wire (99.9%) was obtained from Alfa Aesar, and treated with aqua regia prior to use in all cases. Titanium foil (99.7%, trace metal basis) was obtained from Sigma Aldrich, and treated with concentrated hydrochloric acid prior to use.

General Electrochemical Methods. All electrochemical experiments were conducted at ambient temperature (21 ± 1 ˚C) using a Biologic VSP 16-channel potentiostat and a three-electrode electrochemical cell with a porous glass frit separating the working and auxiliary compartments. Unless otherwise stated, a platinum mesh was used as the counter electrode. Hg/HgO and Ag/AgCl reference electrodes were use for experiments conducted in alkaline and acidic electrolytes, respectively, whereas a Ag wire pseudo-reference electrode was used for experiments conducted in non-aqueous electrolyte. Hg/HgO reference electrodes were stored in 1 M KOH solution in between measurements and were periodically checked relative to pristine reference electrodes to ensure against potential drift. Electrode potentials were converted to the reversible hydrogen electrode (RHE) scale using E(RHE) = E(Hg/HgO) + 0.094 V + 0.059(pH) V. Ag/AgCl electrodes were stored in saturated NaCl solution in between measurements and were periodically checked relative to pristine reference electrodes to ensure against potential drift. Electrode potentials were converted to the RHE scale using E(RHE) = E(Ag/AgCl) + 0.197 V + 0.059(pH) V. Non-aqueous electrochemical measurements were conducted using a Ag wire pseudo-reference electrode.

Synthesis of Pyrazine-Modified Glassy Carbon Electrodes. Glassy carbon rotating disk electrodes, 5 mm diameter, were polished by hand against an alumina slurry using a circular motion for ~30 seconds following by sonication in Milli-Q water for 3 min. This process was repeated in sequence using 1.0 μm, 0.3 μm, and 0.05 μm alumina slurries. To further clean the glassy carbon electrode surface and expose a high population of quinone moieties the electrode were briefly anodized via potentiostatic electrolysis at 3.5 V vs RHE for 10 seconds in 0.1 M H_2SO_4.[1] Electrodes were subsequently washed with copious amount of water and ethanol prior to electrochemical evaluation or further functionalization. Surface functionalization was carried out by immersing glassy carbon electrodes in ~ 10 ml of N_2 sparged ethanol containing 50 mM of the desired *ortho*-phenylenediamine derivative, **1'**, **2'**, **3'** or **4'** (3,4-diaminobenzenecarboxylic

acid). The reaction vessel was subsequently heated under N_2 for 12 hours at 60˚C. Upon cooling, electrodes were washed with copious amount of pure ethanol and subsequently treated with 0.1 M $HClO_4$ for 3 hours to hydrolyze adventitious imine linkages formed on the surface. To avoid possible photoreactions, all reactions were conducted in the dark. Following acid treatment, electrodes were rinsed with copious amounts of pure water and subsequently transferred to the desired electrolyte solution for electrochemical measurements or stored in air for analytical measurements. Unmodified control electrodes used for the comparison in Figure 3a were prepared used the same procedure described above but with exclusion of the phenylenediamine in the reaction mixture.

Synthesis of Pyrazine-Modified High-Surface Area Carbons. Prior to functionalization, high surface area Monarch 1300 carbon was continuously washed with ethanol for ~12 hours under an N_2 atmosphere using a Soxhlet extractor. Following this washing step, 0.2 g of carbon powder was dispersed in 20 ml of ethanol containing 0.5 mmol of the desired phenylenediamine derivative (25 mM concentration). The reaction vessel was held at 60˚C overnight under an N_2 atmosphere. Upon cooling the reaction mixture, the carbon powder was filtered and washed with 500 ml of ethanol and 200 ml of water. The carbon powder was subsequently dispersed in an aqueous 0.1 M $HClO_4$ solution and allowed to react overnight. To avoid possible photoreactions, all reactions were conducted in the dark. Following acid treatment, the carbon powder was filtered and washed with 1000 ml of pure water. The washed carbon powder was then transferred to the thimble of a Soxhlet extractor and washed continuously with refluxing ethanol for 1 day and refluxing *ortho*-dichlorobenzene for 2 days under an N_2 atmosphere. To remove residual *ortho*-dichlorobenzene, the sample was subsequently washed with copious amounts of ethanol and dried overnight in *vacuo*. The sample was then stored in air in the dark prior to data collection.

XPS Measurements. The X-ray photoelectron spectra were collected using a Physical Electronics Model PHI Versaprobe II with a hemispherical energy analyzer and a non-monochromated X-ray source (Aluminum Kα, 1486.6 eV). Samples were prepared by affixing glassy carbon disk electrodes and molecular films to the sample stage using conductive Cu tape. Data were collected using a 200 μm, 50 W focused X-ray beam at a base pressure of 7×10^{-7} Pa. High resolution scans centered over peaks of interest were collected with a pass energy of 117.4 eV and a step size of 0.7 eV. The C 1s peak arising from adventitious hydrocarbons was assigned the energy value of 285.0 eV and used as an internal binding energy reference.

XPS Curve Fitting. XPS fitting was conducted using XPSPEAK 4.1. Shirley line was used for the background collection. All the spectra were fitted to asymmetric Gaussian functions[2] using the following equation:

$$G(x,p,w,h,TS,TL) = h[e^{-\ln(2)Q} + TS[1 - e^{-\ln(2)Q}] * e^{-\frac{6.9}{TL}Q}],$$

where $Q = [\frac{2(x-p)}{w}]^2$, x: binding energy, p: peak position, w: FWHM, h: peak height, TS and TL are parameters describing the asymmetric tail. Peak fitting was carried out by optimization of p, h, w and then optimization of asymmetric parameters TS and TL. Fitting results and fit qualities (χ^2) are shown in Figures 1a and S1 and Table S1.

X-ray Absorption Spectra. Nitrogen K-edge X-ray absorption spectra were collected at bending magnet beamline 6.3.1 (1011 photons/s) at the Advanced Light Source at Lawrence Berkeley National Laboratory. Powder samples were pressed into In foil and mounted to a Cu sample plate. Incident radiation was tuned with a variable line spacing plane grating monochromator (VLS-PGM) and its intensity monitored with a gold mesh upstream of the samples. Spectra were collected in total electron yield (TEY) mode. The baselines were fit to third-order polynomials and removed, and intensities were normalized to the peak near 408 eV. The nitrogen K-edge spectrum of polycrystalline h-BN powder was collected in TEY mode and used for energy calibration. XANES spectra are shown in Figures 1b and S3.

Voltammetric Measurements of Modified Glassy Carbon Electrodes. Native and modified glassy carbon rotating disk electrodes were prepared as described above and transferred to 0.1 M KOH electrolyte. Linear sweep or cyclic voltammograms were initiated at the open circuit potential and swept in the negative direction while rotating the electrode at a rotation rate of 2000 RPM. Uncompensated resistances were measured prior to each experiment and typically ranged from 40-50 Ω, leading to maximum uncompensated. Ohmic losses of ~2 mV for the CVs. As such, all CV scans were recorded without *i*R compensation. Cyclic voltammetry scans recorded in N_2-saturated 0.1 M KOH produced the data shown in Figure 2, Figure 4 and Figure S4. Redox waves correspond to surface bound pyrazine units were found to have peak currents linearly proportional to the scan rate (representative data is shown in Figure S5). The population of electroactive surface bound pyrazines was estimated by integration of redox waves observed in slow scan (5 mV/s) cyclic voltammograms (Figure S7). Linear sweep voltammetry scans of oxygen reduction catalysis were recorded in O_2-saturated 0.1 M KOH without *i*R compensation and produced the data shown in Figures 3, 4, S8, S11, and S17. Catalytic onset potential was taken to be the potential at which the LSV displayed −10 μA cm^{-2} current density.

Determination of Surface Concentration of Pyrazine Units. In order to obtain accurate values of the surface concentration of the pyrazine units, we determined the surface roughness of the anodized glassy carbon electrodes using double-layer capacitance measurements recorded in N_2-saturated acetonitrile electrolyte containing 0.1 M $N(Bu)_4PF_6$. These measurements were conducted in non-aqueous electrolyte to minimize proton coupled pseudo-capacitive currents that have been shown to artificially inflate surface area measurements.[3] Double-layer capacitance measurements were conducted by sweeping the potential over a 100 mV window centered at the open circuit potential using a range of sweep rates spanning 0.5 to 5 mV/s. These low sweep rates were chosen to minimize convolution from ion transport limitations within the electrode microstructure. A representative plot of double layer capacitive current versus sweep rate is shown in Figure S6 and yields the surface capacitance values shown in Table S3. This value was used to calculate the area normalized surface concentrations of pyrazine units using the following equation,

$$\Gamma_{GCP} = \frac{Q_{GCP} \times C_{dl-planar}}{C_{dl} \times nF}$$

where $\mathbf{\Gamma}_{GCP}$ is the surface concentration of the pyrazines unit in moles per electroactive cm^2, Q_{GCP} is the aggregate integrated charge density of the redox waves for surface pyrazines in the absence of O_2 (Figure S7), F is Faraday's constant, n is the number of electrons, taken to be 2 based on the known two electron redox chemistry of pyrazines,[4] C_{dl} is the double layer

capacitance measured via variable scan-rate voltammetry, and $C_{dl\text{-}planar}$ is the theoretical double layer capacitance of a planar glassy carbon electrode, taken to be 20 μF/cm^2 based on literature precedent.[5] Surface concentration data for all electrodes is shown in Table S3.

Electrolyte Purity Dependence of Oxygen Reduction Catalysis. To evaluate whether trace metal ion impurities in the electrolyte impact oxygen reduction catalysis, **1** was evaluated in native 0.1 M KOH (Figure S8, black) and 0.1 M KOH purified of metal ion impurities by two independent methods: pre-electrolysis and metal ion chelation. Pre-electrolyzed solutions were prepared by potentiostatic electrolysis of an N_2-saturated 0.1 M KOH electrolyte bath at −1 V for 1 hour using a glassy carbon disk working electrode rotated at 2000 RPM. Electrode rotating increases the rate of mass transport to the surface accelerating electrodeposition of metal ion impurities. The working electrode was removed from the electrolyte solution under polarization to ensure removal of any electrodeposited metal ions, after which **1** was evaluated for oxygen reduction catalysis (Figure S8, green). Independently, the 0.1 M KOH was purified by metal ion chelation using an iminodiacetate resin (Chelex® 100) known to have a high affinity for a broad array of metal ions. Prior to use, the Chelex resin was regenerated by treatment with 1 M HCl overnight, followed by washing with 5 liters of MilliQ water. Subsequently, 1 liter of 1 M KOH was added to the Chelex resin to generate the anionic active form and was then washed with one 1 liter of MilliQ water to remove residual base. The purified 0.1 M KOH solution was prepared by stirring the native 0.1 M KOH with the regenerated Chelex resin overnight and subsequent filtering. **1** was evaluated for oxygen reduction catalysis in this purified medium and the produced the data in Figure S8, red. In all cases, the data overlaid within ± 5 mV.

Potentiostatic Tafel Data Collection. Steady-state current-potential (Tafel) data were collected by conducting controlled-potential electrolysis of modified glassy carbon rotating disk electrodes in O_2-saturated 0.1 M KOH electrolyte at a variety of potentials spanning the foot of the catalytic wave observed in Figure 3. Typical values of R_u ranged from 40-50 Ω, leading to uncompensated Ohmic losses of < 5mV, which were neglected during data processing. For the higher overpotential data points, activation-controlled currents were determined by extrapolating Koutecky-Levich (K-L) plots to infinite rotation rate. The rotation rate of the electrode was varied between 400 to 2025 RPM, and representative K-L plots are shown in Figure S10. In all cases, catalytic currents reached steady state within 1 minute, and the endpoint current was taken as the steady state value. The data shown in the Tafel plots (Figure 3) are the average and standard deviation of 3 independently prepared electrodes and representative data overlays of independent electrode preparations are shown in Figure S9. The Tafel data were normalized by the number of electroactive pyrazine units by dividing the raw activation-controlled catalytic current by the total integrated charge of the redox wave(s) observed in the absence of O_2 to generate the per-site turnover frequency plots shown in Figure 3. These data are also the average and standard deviation of 3 independently prepared electrodes.

Estimation of TOF of Polycrystalline Ag. Polycrystalline Ag disk electrodes, 5 mm diameter, were polished by hand against an alumina slurry using a circulation motion for ~30 seconds, following by sonication in Milli-Q water for 3 min. This process was repeated in sequence using 1.0 μm, 0.3 μm, and 0.05 μm alumina slurries. The surface site density of Ag atoms was taken as one half of the integrated charge required to deposit a monolayer of Cd atoms on the surface. This value was determined by under potential deposition (UPD) of Cd onto the polycrystalline silver electrode.[6] Prior to ORR catalysis, cyclic voltammograms were recorded at 5 mV/s in N_2-

saturated 0.5 M Na_2SO_4 electrolyte containing 0.01 M H_2SO_4 and 0.01 M $CdSO_4$. The broad wave at −0.5 V vs Ag/AgCl was integrated to yield a surface charge for Cd UPD of 183 μC/cm^2. Since two electrons are required to reduce each Cd^{2+} ion to Cd metal, and Cd UPD is known to form a Cd monolayer on Ag,[6] this value corresponds to a Ag site density of 9.5×10^{-10} mol/cm^2. Following the surface area measurement, the electrode was washed with Milli-Q water and then transferred to 0.1 M KOH electrolyte. Steady-state Tafel data was collected using the procedure described above and the data were normalized to the surface site density of Ag by dividing the raw activation-controlled catalytic current by one half of the integrated charge of the Cd UPD wave to generate the per-site turnover frequency plot shown in Figure 3b. The Cd UPD measurement was repeated following electrolysis and revealed the same UPD charge density indicating that the surface area was preserved over the course of ORR catalysis.

Rotating Ring Disk Electrode Linear Sweep Voltammetry. The Faradaic efficiency for four-electron reduction of O_2 to H_2O was calculated via rotating ring disk electrode (RRDE) voltammetry using a Pine E6 RRDE containing a Pt ring electrode surrounding the modified glassy carbon disk electrode under investigation. While rotating the electrode at 2000 RPM, CV scans were initiated at the open circuit potential while the ring electrode was held at a constant polarization of 1.2 V vs RHE. These CV scans were invariant with cycle number and produced the representative data shown in Figure S11. The Faradaic efficiency at a given potential was determined using the following equation,

$$FE_{H_2O} = \frac{i_d - \frac{i_r}{CE}}{i_d}$$

where FE_{H2O} corresponds to the Faradaic efficiency for four-electron oxygen reduction, i_d is the disk current, i_r is the background-corrected ring current, and CE is the collection efficiency of the RRDE. The background ring current was taken as the steady state ring current measured while the disk electrode was held at open-circuit. Prior to the measurement, a collection efficiency of 0.2 for this rotating ring disk electrode was determined by potentiostatically reducing ferricyanide while concurrently back oxidizing the generating ferrocyanide on the ring electrode. The calculated Faradaic efficiencies for four-electron reduction of O_2 are shown in Figure S11b.

Voltammetry of Water-Soluble Pyrazines. Polished glassy carbon disks served as working electrodes. CV scans of molecules bearing pyrazine units were recorded without *i*R compensation in N_2-saturated 0.1 KOH electrolyte and generated the data shown in the Figure 4a. GCP **4** (shown below), which bears the same carboxylate functional group, was also prepared to provide a fair comparison. The structure of 4 is shown in the scheme below. Peak currents were found to scale linearly with the square root of the scan rate for pyrazine (Figure S14), and quinoxaline-6-carboxylic acid (Figure S15) indicating a freely diffusing species. For dibenzo[a,c]phenazine-2-carboxylic acid, peaks currents scaled neither as a linear nor square root function of the scan rate (Figure S16), indicating contributions to the CV wave from adsorbed and diffusing species. The oxygen reduction activity of the molecules was probed in O_2-saturated 0.1 KOH electrolyte using a polished glassy carbon disk electrode rotated at 2000 RPM and produced the data shown in Figure 4b. The catalytic onset potential was taken to be the potential at which the LSV displayed −10 μA cm^{-2} current density. Increasing concentrations of quinoxaline-6-carboxylic acid were found to progressively passivate the electrode surface (Figure S17).

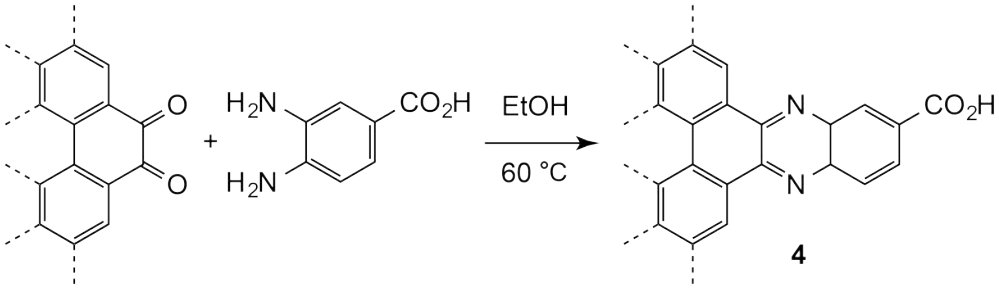

Long-Term Electrode Stability. The long-term stability of the modified electrodes was evaluated by controlled potential electrolysis in O_2-saturated 0.1 M KOH electrolyte. Electrolysis was conducted in a single-compartment 3-electrode cell containing a modified glassy carbon rotating disk electrode rotated at 2000 RPM, a Ti foil counter electrodes, and a Hg/HgO reference electrode. The Ti foil (~ 4cm^2) counter electrode was treated with concentrated hydrochloric acid prior to use. A single compartment cell was used to prevent pH gradients from developing over the course of prolonged electrolysis. Long-term stability traces are shown in Figure S8 for **1** and **3**.

Fabrication of High-Surface Area Carbon-Coated Disk Electrodes. 0.1 ml of 5% Nafion solution, 0.1 ml of ethanol, 1.8 ml of water, and 10 mg of functionalized carbon powder were combined and resulting dispersion was sonicated for 30 minutes to generate a homogeneous colloidal ink. 20 µl of this dispersion was dropcast onto a 5 mm diameter glassy carbon rotating disk electrode and dried at 60˚C to form a well-adhered film. This procedure led to a carbon mass loading of ~0.5 mg cm^{-2}.

Synthesis and Characterization of Molecular Precursors and Model Compounds.

General Characterization Methods:

^{1}H and ^{13}C NMR spectra were recorded on a Varian 500 MHz spectrometer. All chemical shifts are reported in ppm and are referenced to tetramethylsilane (TMS) utilizing residual ^{1}H or ^{13}C signals of deuterated solvents as internal standards. ^{19}F NMR spectra were recorded on a Varian 300 MHz spectrometer. ^{19}F chemical shifts are reported in ppm and are referenced to $CFCl_3$ utilizing 2,2,2-trifluoroethanol as an internal standard. High-resolution mass spectra were obtained using a Bruker Daltonics APEXIV 4.7 Tesla FT–ICR–MS using ESI or DART ionization. Elemental analyses were carried out by Robertson Microlit Laboratories, Inc., Ledgewood, NJ.

Synthesis of 3':

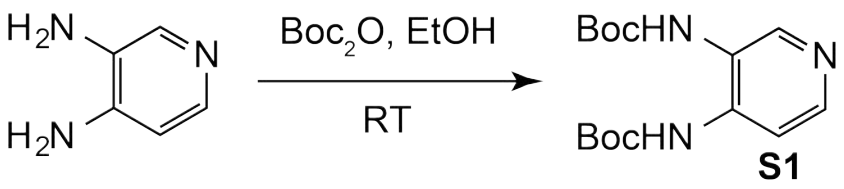

The synthesis was conducted according to the modified literature procedure.[7] 1.09 g (10 mmol) of 3,4-diaminopyridine was dispersed in 20 ml of ethanol. 5.45 g (25 mmol) of di-*t*-butyl

dicarbonate (Boc_2O) was added to the ethanol solution and allowed to react at room temperature overnight. The solution color changed from transparent to yellow with visible bubble formation. Subsequently, the solution was evaporated to give a crude product as a yellow oil. The crude product was purified by silica column chromatography (2:8 ethanol/CH_2Cl_2). The purified product was dried *in vacuo* overnight to give 0.58 g (19%) of a pale yellow powder, **S1**.

^{1}H NMR (500 MHz, CD_2Cl_2, δ): 8.09 (s, 1H), 8.01 (d, 1H), 7.59 (d, 1H), 6.78 (s, 2H) 1.51 (s, 18H). **^{13}C NMR (500 MHz, CD_2Cl_2, δ):** 153.1, 141.7, 139.6, 134.5, 133.3, 114.8, 81.4, 28.4. **HRMS (ESI-M+):** theoretical [M+H] 310.1761, experimental 310.1775.

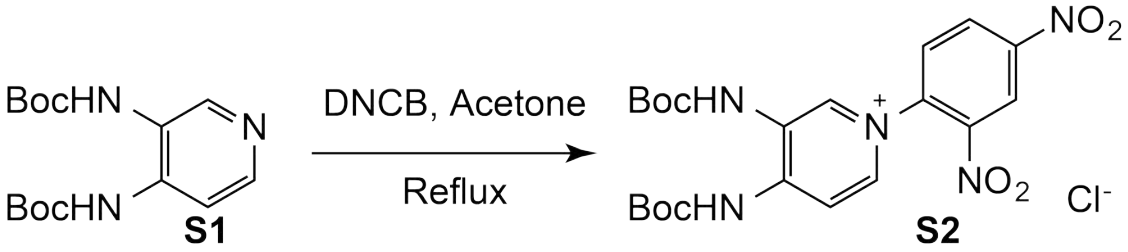

Preparation of the Zincke salt (shown above) was conducted according to a modified literature procedure.[8] 3.09 g (10 mmol) of **S1** and 2.22 g (11 mmol) of 2,4-dinitrochlorobenzene (DNCB) were dissolved in 20 ml of acetone. The solution was heated to reflux under N_2 atmosphere. Following an overnight reaction, the resulting orange solid was filtered, washed with 10 ml of acetone and dried to yield 1.43 g (56%) of **S2**.

^{1}H NMR (500 MHz, DMSO-d^6, δ): 9.01 (s, 1H), 8.83 (d, 1H), 8.58, (s, 1H), 8.33 (d, 1H), 8.24 (d, 1H) 7.99 (s, 1H), 7.65 (d, 1H), 1.54 (s, 18H). **^{13}C NMR (500 MHz, DMSO-d^6, δ):** 151.5, 150.1, 148.0, 145.9, 141.5, 141.0, 140.6, 134.1, 132.2, 123.7, 120.2, 109.6, 88.4, 87.3, 30.4, 29.8.

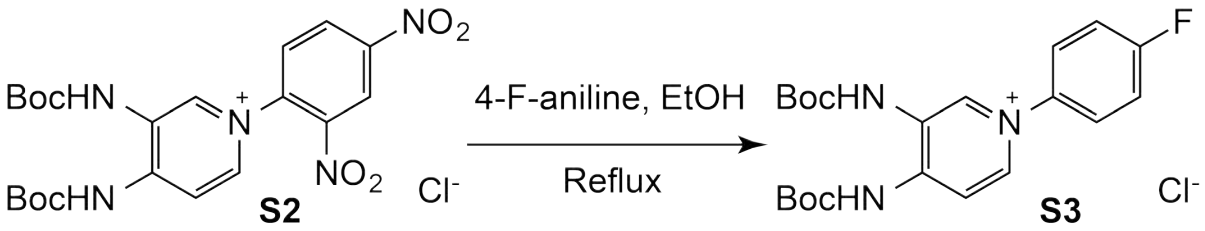

2.55 g (5 mmol) of **S2** was dispersed in 10 ml of 4-fluoroaniline (100 mmol) and 60 ml of ethanol. The solution was then heated to reflux under an N_2 atmosphere overnight. Upon cooling, the reaction mixture was concentrated to generate ~15 ml of a red oil. 5 ml of ethanol was then added to precipitate an orange solid. The orange solid was filtered, washed with 5 ml of ethanol, and dried *in vacuo* to yield 0.91 g (41%) of **S3**.

^{1}H NMR (500 MHz, CD_2Cl_2, δ): 9.92 (s, 1H), 9.18 (s, 0.6H), 8.19 (d, 1H), 7.38 (d, 2H), 7.23 (d, 2H), 7.03 (d, 1H), 1.53 (s, 18H) . **^{13}C NMR (500 MHz, CD_2Cl_2, δ):** 162.8, 160.9, 147.6, 137.6, 133.2, 131.3, 130.1, 128.1, 128.0, 123.9, 117.6, 117.4, 116.1, 88.2, 86.9, 30.3, 29.7. **^{19}F NMR (300 MHz, $CDCl_3$, δ):** -108.3.

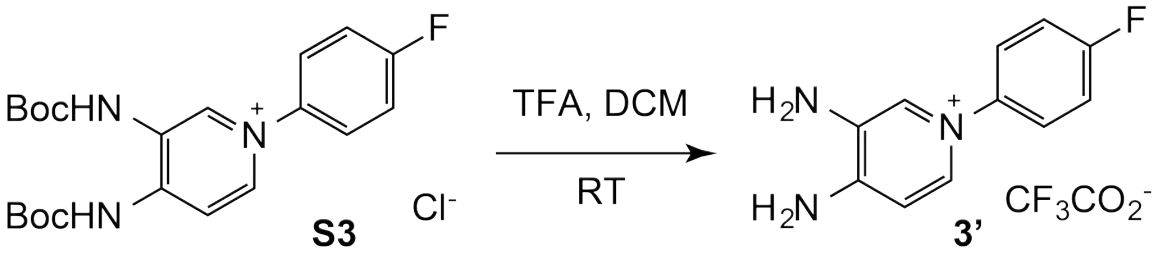

0.40 g (10 mol) of **S3** was dissolved in 20 ml of a 1:1 mixture of trifluoroacetic acid and dichloromethane and allowed to react at room temperature for 3 hours. Subsequently, the solvent was removed by rotary evaporation and the crude product was recrystallized from an ethanol/dichloromethane mixture, yielding orange crystals of **3'** as a mixture of chloride and trifluoroacetate salts 0.21 g (72%).

^{1}H NMR (500 MHz, CD_2Cl_2, δ): 9.86 (s, 1H), 9.14 (s, 0.7H), 8.17 (d, 1H) 7.32 (d, 2H), 7.23 (d, 2H), 7.04 (d, 1H) ppm. **^{13}C NMR (500 MHz, CD_2Cl_2, δ):** 162.9, 160.9, 147.7, 137.6, 133.1, 131.3, 130.2, 128.3, 128.2, 124.1, 117.4, 117.2, 116.2. **^{19}F NMR (300MHz, $CDCl_3$, δ)** 64.7, -114.5. **Elemental analysis:** $C_{24}H_{22}ClF_5N_6O_2$, Calculated: C 51.76, H 3.98, N 15.09, Found: C 52.48, H 3.46, N 14.76.

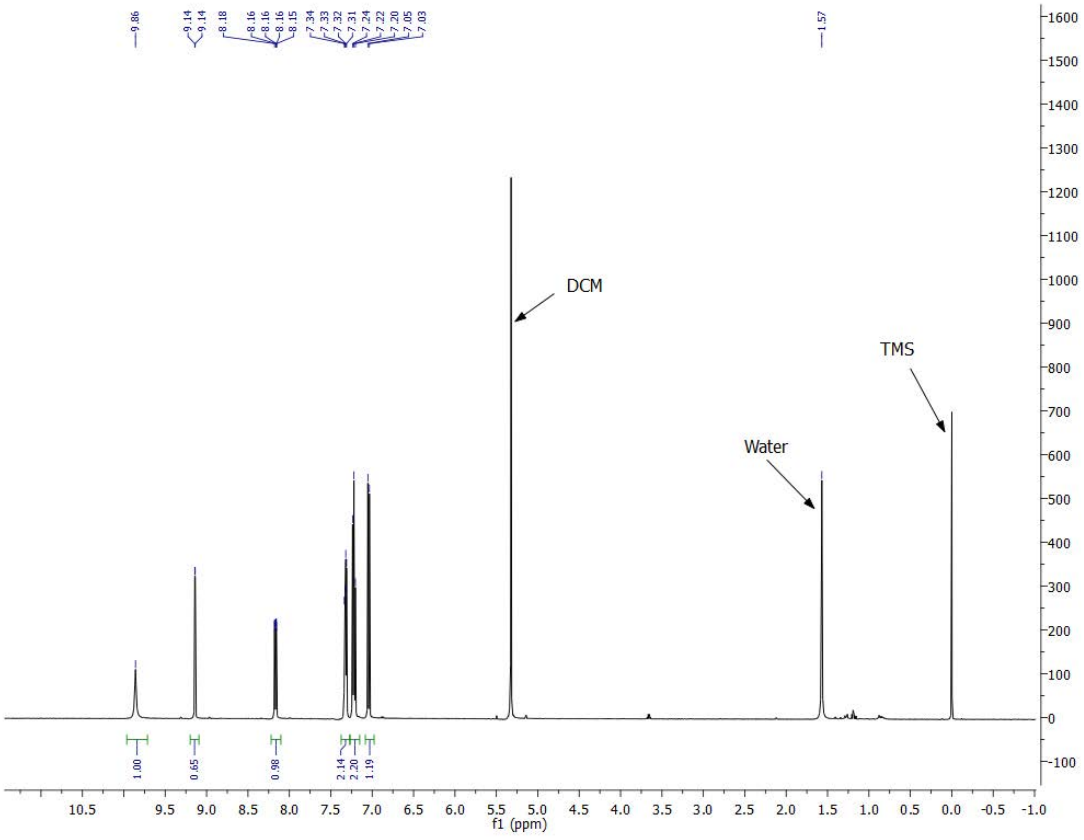

Synthesis of dibenzo[a,c]phenazine-2-carboxylic acid:

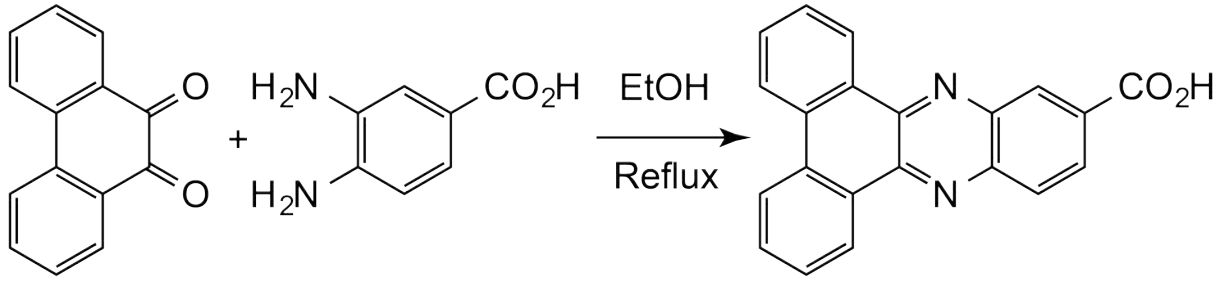

1.04 g (5 mmol) of 9,10-phenanthraquinone and 0.75 g of 3,4-diaminobenzene-1-carboxylic acid (5 mmol) were suspended in 100 ml of ethanol. The reaction mixture was refluxed for 3 hours, and the resulting yellow solid was isolated by filtration. The solid was dispersed in 100 ml of ethanol, and heated to reflux for 30 minutes to dissolve residual starting materials. The solid was filtered hot and dried overnight *in vacuo* to yield 0.52 g (32%) of dibenzo[a,c]phenazine-2-carboxylic acid.

^{1}H NMR (500 MHz, DMSO, δ): 9.29 (d, 2H), 8.86 (s, 1H) 8.81 (d, 2H), 8.41 (t, 2H), 7.92 (m, 2H) 7.85 (t, 2H) ppm. **^{13}C NMR** (N/A – the compound exhibited too low solubility). **Elemental analysis:** Calculated: C 77.77, H 3.73, N 8.64. Found: C 77.44, H 3.40, N 8.66. **HRMS (ESI-MS−):** *m/z* theoretical [M^-] 323.0826, experimental 323.0805

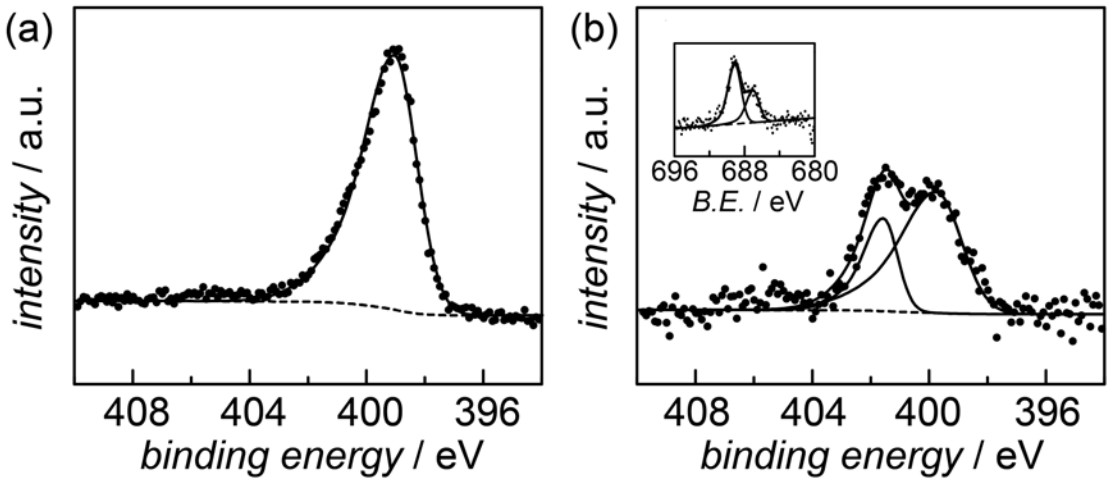

Figure S1. High resolution N 1s XPS scans of **2** (a) and **3** (b). High resolution F 1s XPS scan of **3** (b inset).

Table S1. Fitting parameter for XPS spectra of **1**, **2**, and **3**.

Sample	Nuclei	Peak position / eV	FWHM / eV	TS	TL	χ^2
1	N1s	398.89	2.56	0.5	50	4.55
1	F1s	686.99	1.62	0.2	50	2.96
2	N1s	399.04	2.24	0.5	50	3.72
3	N1s	399.61 (67.4%) 401.71 (32.6%)	2.41 1.69	0.5	50	2.00
3	F1s	686.95 (34.0%) 689.13 (66.0%)	1.633 1.944	0.2	50	1.57

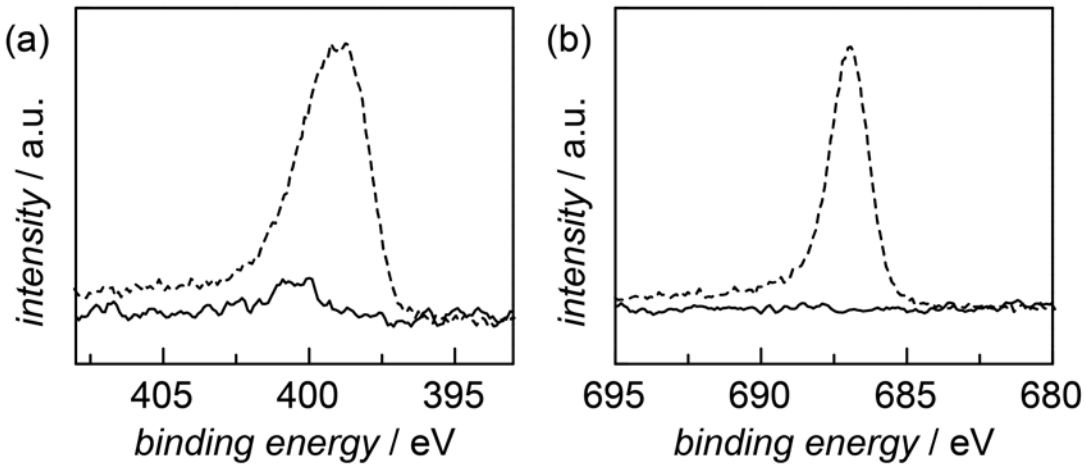

Figure S2. High resolution XPS scans of N 1s (a) F 1s (b) regions for an unmodified glassy carbon electrode (solid line) and **1** (dashed line).

Table S2. Elemental analysis of Monarch 1300 and Monarch 1300 treated with **1'**.

#	C%	H%	N%
Monarch 1300	86.87	0.52	0.11
Monarch 1300 - **1'**	89.72	1.13	1.31

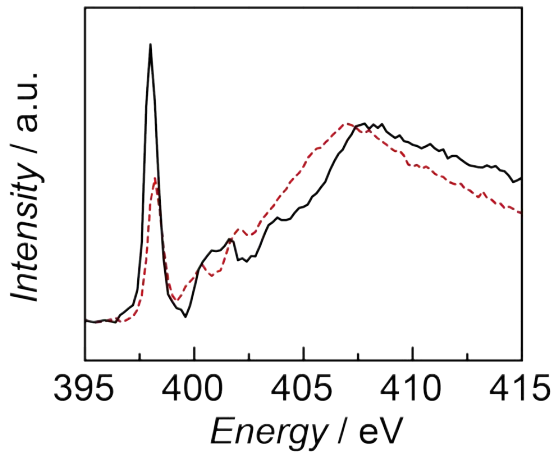

Figure S3. N K-edge XANES of **1'**-treated Monarch (black) and **1'** (4-fluoro-1,2-phenylenediamine) (red dotted line).

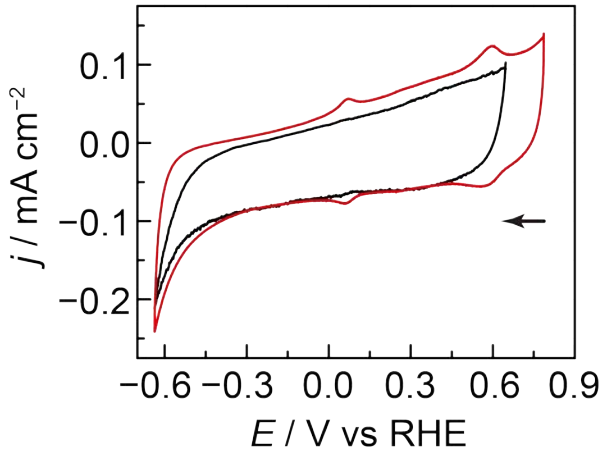

Figure S4. Representative cyclic voltammograms of unmodified glassy carbon (black) and **3** (red) recorded in N_2-saturated 0.1 M KOH electrolyte at a scan rate of 5 mV/s. Arrow indicates the direction of scan initiated from the open circuit potential.

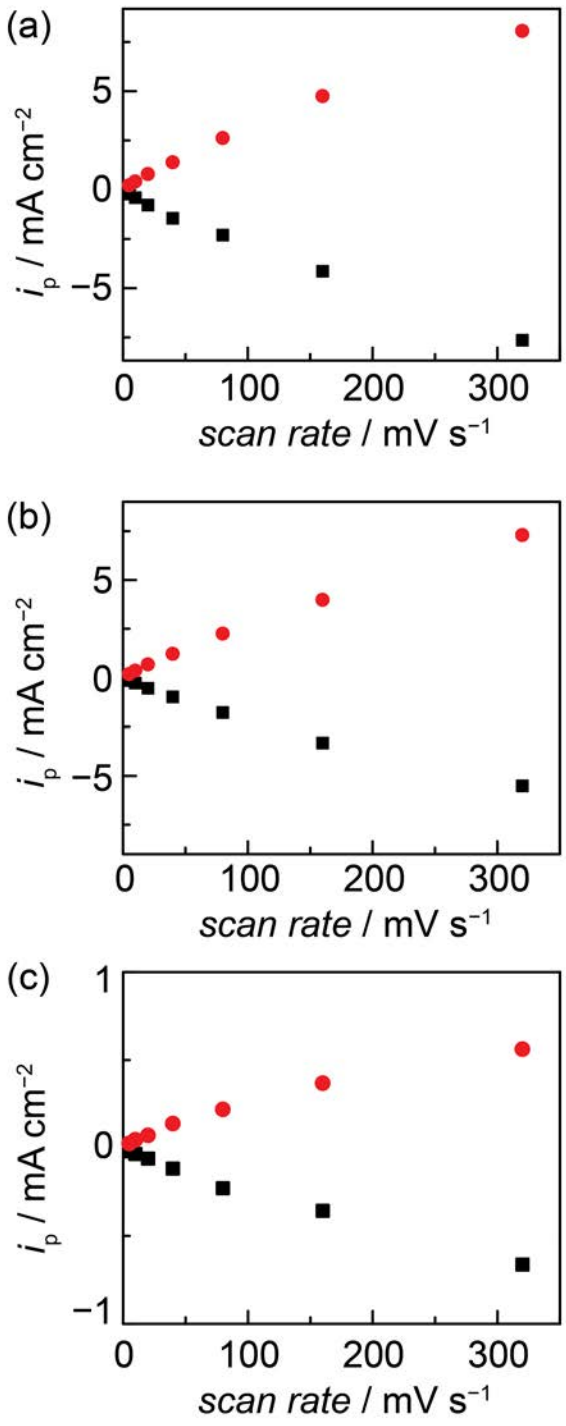

Figure S5. Scan rate dependence of anodic (red) and cathodic (black) peak currents for **1** (a), **2** (b), and **3** (c).

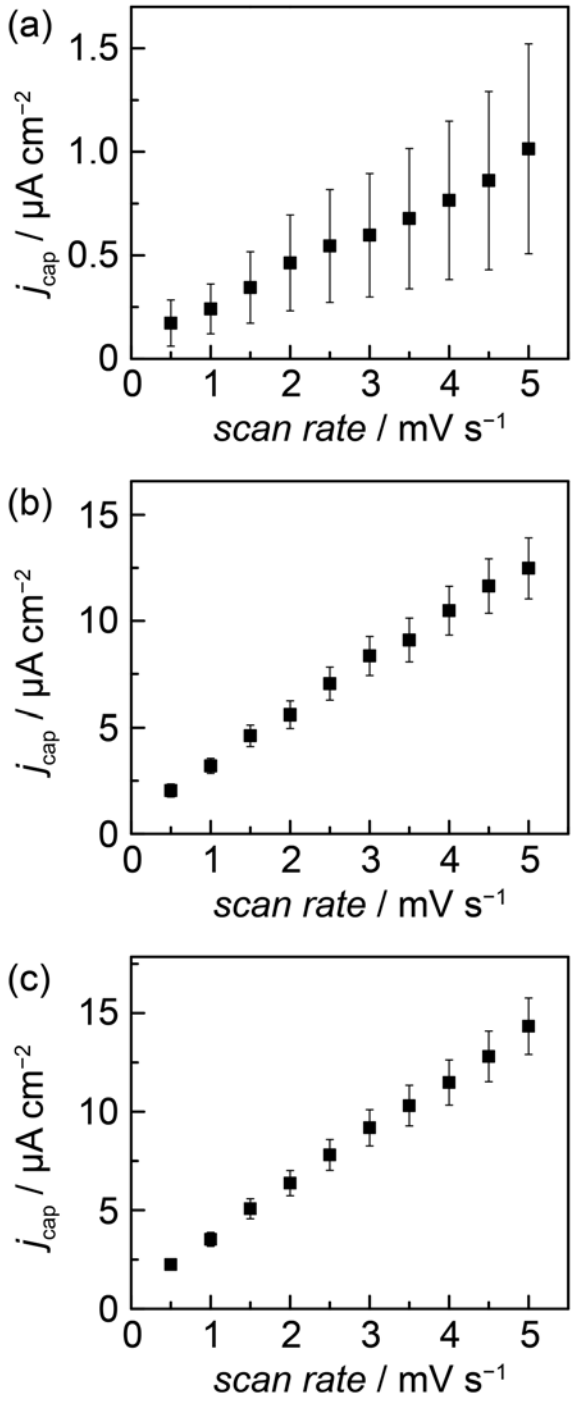

Figure S6. Representative double layer capacitance measurements for polished glassy carbon (a), unmodified anodized glassy carbon (b), and **1** (c). Plots were obtained by taking the capacitive current (j_{cap} = (j_a-j_c)/2) recorded in cyclic voltammograms in N_2-saturated 0.1 M $N(Bu)_4PF_6$ acetonitrile electrolyte.

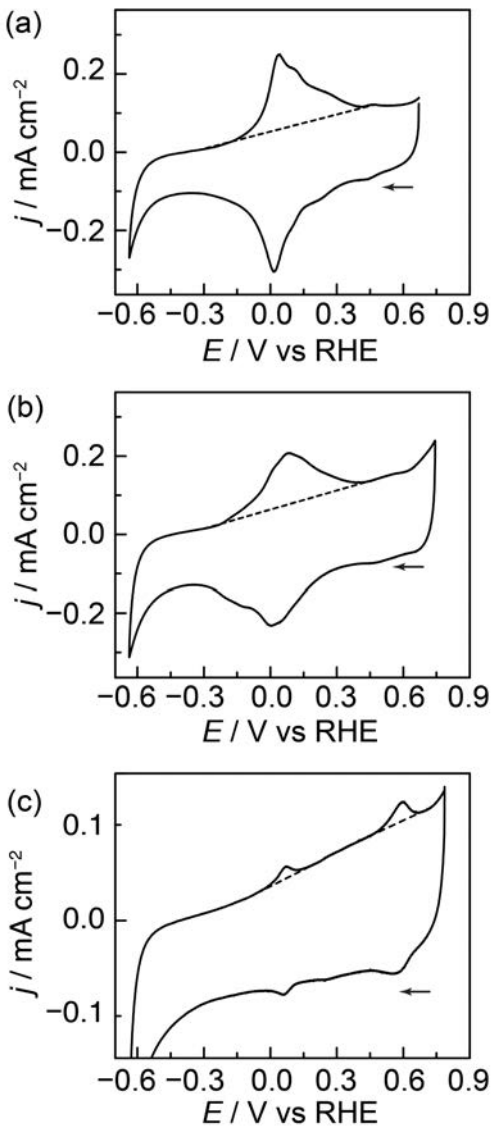

Figure S7. Representative cyclic voltammograms of **1** (a), **2** (b), and **3** (c) recorded in N_2-saturated 0.1 M KOH electrolyte by 5 mV/s. Dotted lines denote baselines for peak integrations.

Table S3. Electrochemical parameters used to calculate the surface concentration of pyrazine moieties. Based on literature precedent,[5] the double layer capacitance of a planar glassy carbon surface, $C_{dl\text{-}planar}$, was taken as 20 μF cm^{-2}. The surface concentration of pyrazine units was calculated assuming that each site underwent a net two-electron reduction under N_2.

Sample	Double-layer capacitance, C_{dl}	Integrated charge, Q_{GCP}, of surface pyrazine redox waves	Surface concentration of pyrazine units, $\mathbf{\Gamma}_{GCP}$
Polished glassy carbon	190 ± 100 μF cm^{-2},	N/A	N/A
Anodized glassy carbon	2.4 ± 0.4 mF cm^{-2}	N/A	N/A
1	2.9 ± 0.3 mF cm^{-2}	7.3 ± 0.8 mC cm^{-2}	0.26 ± 0.04 nmol cm$^{-2}_{real}$
2	2.8 ± 0.3 mF cm^{-2}	6.6 ± 0.6 mC cm^{-2}	0.24 ± 0.03 nmol cm$^{-2}_{real}$
3	2.9 ± 0.2 mF cm^{-2}	387 ± 61 μC cm^{-2}	14 ± 2 pmol cm$^{-2}_{real}$

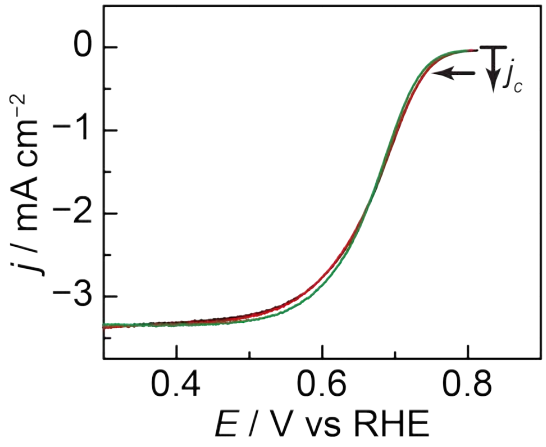

Figure S8. Linear sweep voltammograms of **1** in O_2-saturated native (black), Chelex-treated (red), pre-electrolyzed (green) 0.1 M KOH electrolyte. Data were recorded on a rotating disk electrode at 2000 RPM at a scan rate of 5 mV/s. Observed potential differences are within 5 mV.

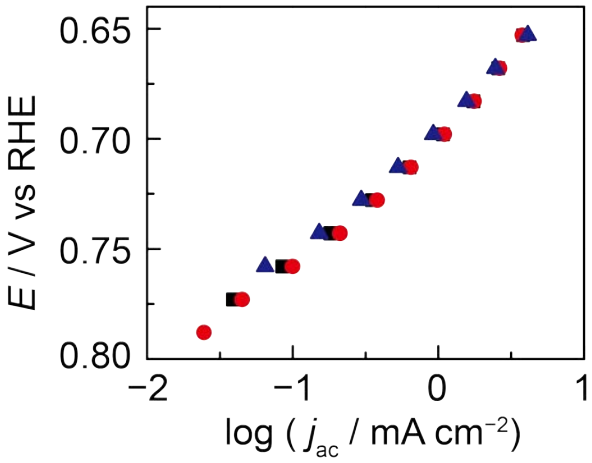

Figure S9. Representative, potentiostatic Tafel plots of **1** for three-independently prepared electrodes recorded in O_2-saturated 0.1 M KOH aqueous electrolyte.

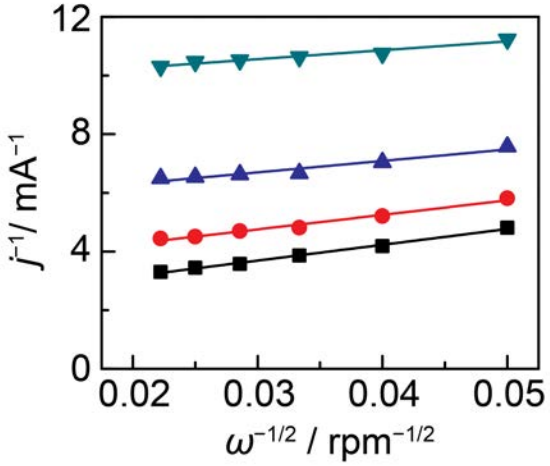

Figure S10. Representative Koutecky–Levich plots of **1**, polarized at 0.72 (▼), 0.71 (▲), 0.69 V (●), and 0.68 V (■). Data recorded in O_2-saturated 0.1 M KOH electrolyte.

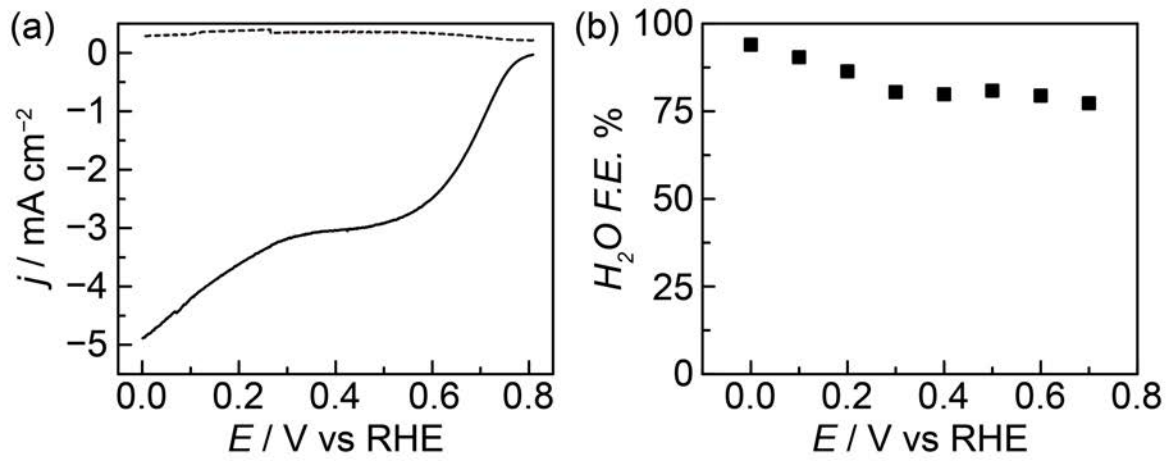

Figure S11. (a) Rotating ring disk linear sweep voltammetry recorded at 5 mV s^{-1} in O_2-saturated 0.1 M KOH electrolyte. Disk current (solid line) for O_2 reduction on **3'**-treated high surface area carbon and ring current of Pt (dotted line) for peroxide oxidation at a rotation rate of 2000 RPM. (b) Steady-state Faradaic efficiency for H_2O production from O_2 reduction.

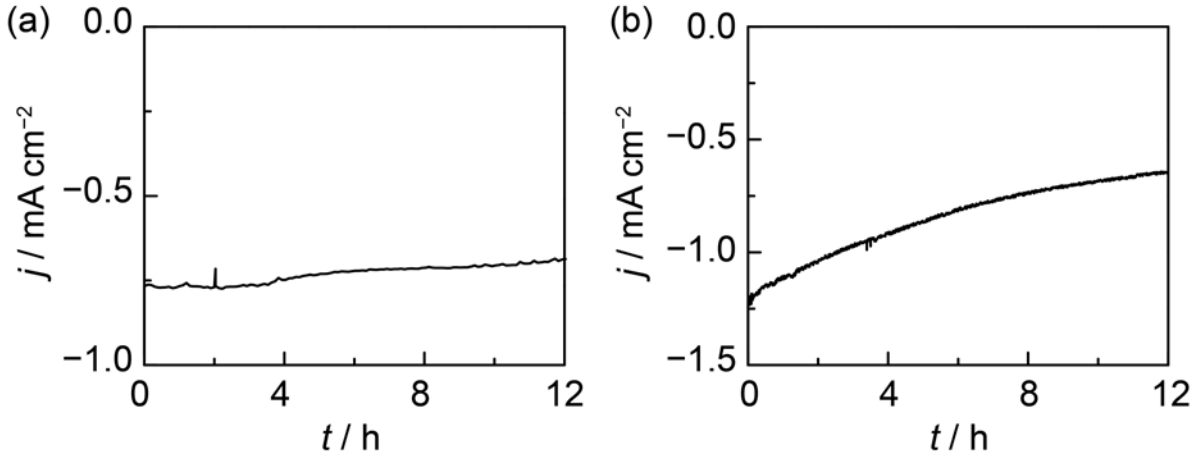

Figure S12. Potentiostatic electrolysis of **1** (a) and **3** (b) recorded in O_2-saturated 0.1 M KOH electrolyte at 0.7 V at a rotation rate of 2000 RPM.

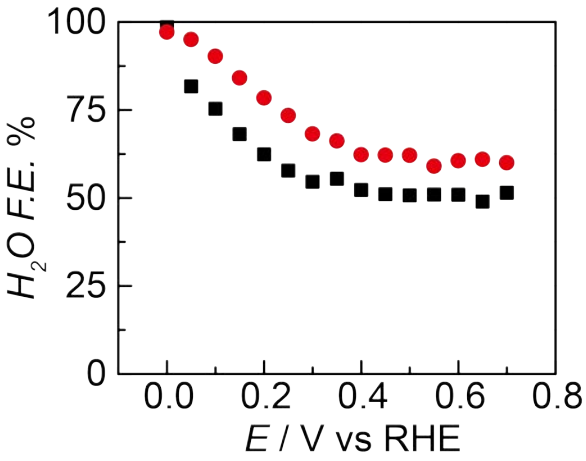

Figure S13. Steady-state Faradaic efficiency for H_2O production from O_2 catalyzed by freshly prepared **3** (black square) and **3** following 12 hours of potentiostatic electrolysis at 0.7 V at a rotation rate of 2000 rpm (red circle).

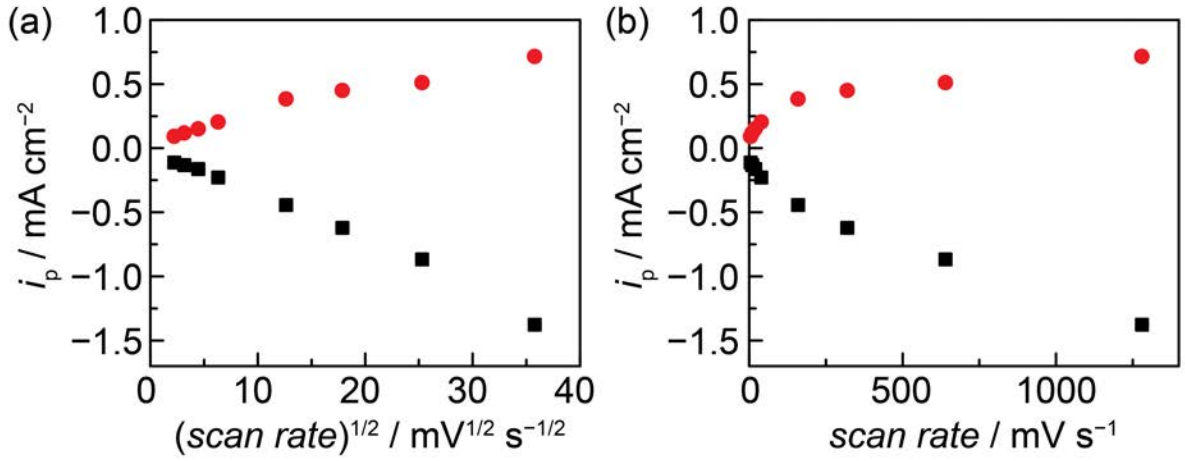

Figure S14. Scan-rate dependence of peak current for pyrazine obtained from cyclic voltammetry in N_2-saturated 0.1 M KOH electrolyte. Red circles and black squares represent anodic and cathodic peak currents, respectively.

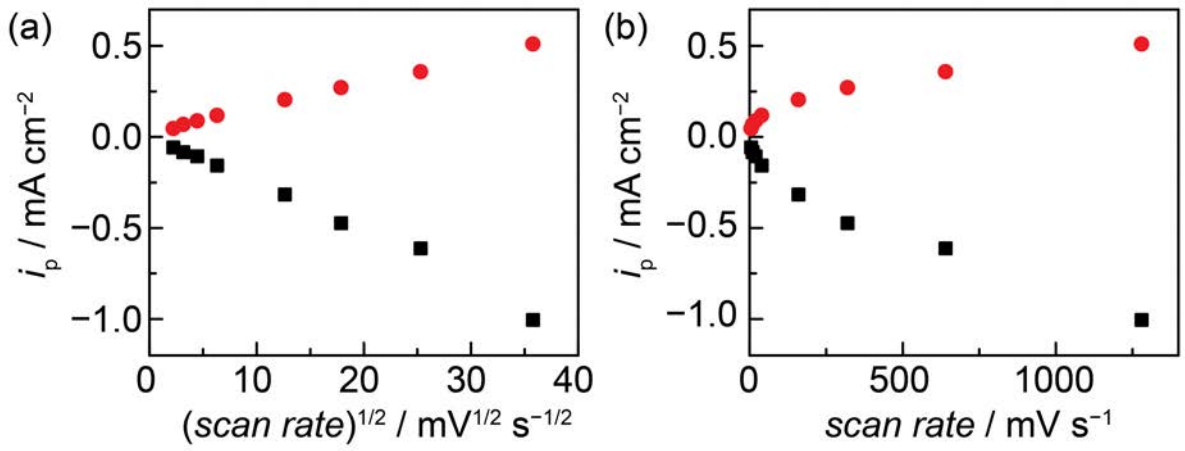

Figure S15. Scan-rate dependence of peak current for quinoxaline-6-carboxylic acid obtained from cyclic voltammetry in N_2-saturated 0.1 M KOH electrolyte. Red circles and black squares represent anodic and cathodic peak currents, respectively.

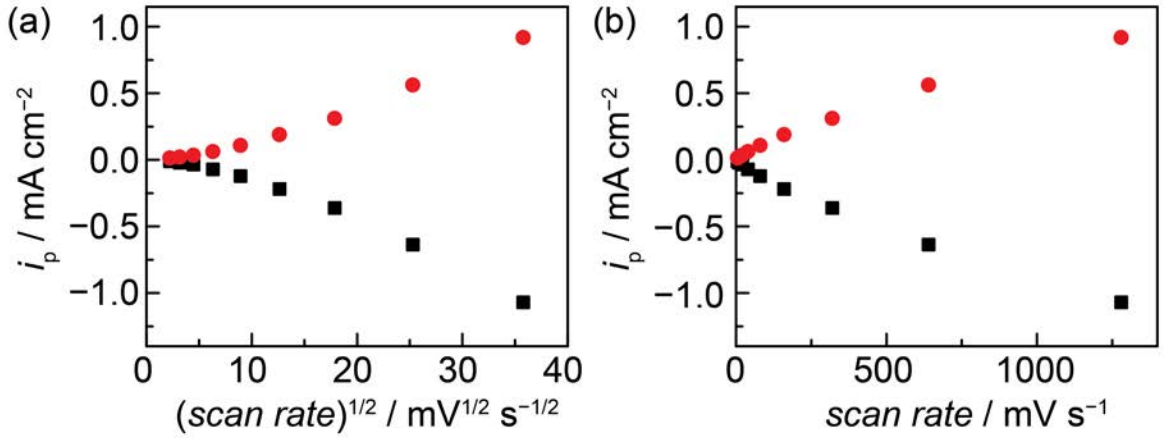

Figure S16. Scan-rate dependence of peak current for dibenzo[a,c]phenazine-2-carboxylic acid obtained from cyclic voltammetry in N_2-saturated 0.1 M KOH electrolyte. Red circles and black squares represent anodic and cathodic peak currents, respectively.

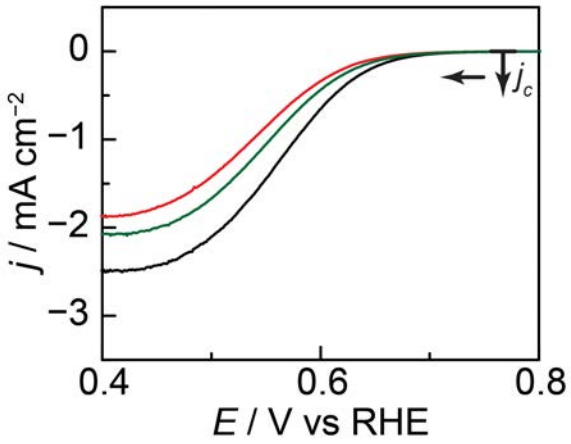

Figure S17. Linear sweep voltammograms (5 mV/s scan rate) of a polished glassy carbon disk electrode in O_2-saturated 0.1 M KOH electrolyte containing 0 (black), 5 (green), and 22 (red) mM quinoxaline-6-carboxylic acid. Data recorded on a rotating disk electrode at 2000 RPM.

---

1) Engstrom, R. C. *Anal. Chem*. **1982**, *54*, 2310-2314.

2) (a) Donicha, S.; Sunjic, M. *J. Phys. C: Solid State Phys*, **1970**, *3*, 285-291. (b) Takahiro, K.; Teraia, A.; Oizumi, S.; Kawatsura, K.; Yamamoto, S.; Naramoto H. *Nuclear Instruments and Methods in Physics Research Section B: Beam Interactions with Materials and Atoms,* **2006**, *242*, 445-447.

3) Koz, J. A.: He, Z.; Miller, A. S.; Switzer, J. A. *Chem. Mater*. **2012**, *24*, 3567-3573.

4) Kaye, R. C.; Stonehill, H. I.; *J. Chem. Soc*. **1952**, 3240-3243.

5) Chmiola, J.; Yushin, G.; Gogotsi, Y.; Portet, C.; Simon, P.; Taberna, P. L. *Science*, **2006**, *313*, 1760-1763.

6) Motheo, A. J.; Machado, S. A. S.; Van Kampen, M. H.; Santos Jr, J. R. *J. Braz. Chem. Soc*, **1993**, *4*, 122-127.

7) Vilaivan, T. *Tetrahedrom Letters* **2006**, *47*, 6739-6742.

8) Wong, Y.-S.; Marazano, C.; Gnecco, D.; Génisson, Y.; Chiaroni, A.; Das, B. C. *J. Org. Chem.* **1997**, *62*, 729–733.